Distinct temporal trajectories of bacterial and fungal networks during agricultural rewilding

Geoffrey Zahn [a,*] , Carl E. Hjelmen [b] , Benjamin J. Wainwright [c,*]

[a] Applied Science Department, William & Mary, 540 Landrum Drive, Williamsburg, VA 23185, USA
[b] Biology Department, Utah Valley University, 800 W University Pkwy, Orem, UT, 84058, USA
[c] Department of Biological Sciences, National University of Singapore, 16 Science Drive 4, 117558, Singapore

HIGHLIGHTS

- Microbial communities in tropical agricultural soils underwent domain-specific reassembly.
- Bacterial and fungal communities followed distinct successional trajectories.
- Shifts in community structure are shaped by key soil nutrients.
- Microbial coalescence is non-uniform.

GRAPHICAL ABSTRACT
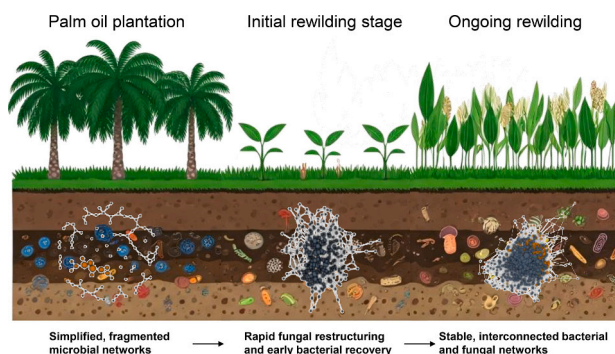
ABSTRACT

Tropical land-use change from native forests to oil palm plantations has created widespread biodiversity loss, soil degradation, and disruption of microbial communities. As rewilding initiatives emerge to restore ecosystem function in post-agricultural landscapes, understanding microbial community assembly, diversity dynamics, and interaction networks is essential for informing effective restoration strategies. However, the pace and predictability of microbial reorganization following intensive monoculture remain poorly understood, particularly in tropical systems. We examined microbial reassembly across a five-year tropical rewilding chronosequence in a former oil palm plantation, using full-length 16S and ITS amplicon sequencing, ecological network modeling, and soil chemistry analyses. Bacterial and fungal alpha diversity increased over time, though with domain-specific trajectories. Generalized dissimilarity models revealed that soil phosphorus and carbon were dominant environmental filters shaping community turnover. Co-occurrence networks showed increasing complexity over time, with bacterial networks becoming progressively more interconnected, while fungal networks exhibited earlier but less sustained restructuring. These patterns suggest that microbial community coalescence during rewilding is asynchronous, structured, and shaped by deterministic environmental filtering and legacy effects of past land use. Our results provide evidence that tropical rewilding can rapidly reorganize soil microbial communities, enhancing diversity, connectivity, and compositional structure within just a few years. Full recovery is likely to require longer time frames, these early trajectories highlight the potential for rewilding to promote functional

* Corresponding authors.
E-mail addresses: gzahn@wm.edu (G. Zahn), carl.hjelmen@uvu.edu (C.E. Hjelmen), ben.wainwright@nus.edu.sg (B.J. Wainwright).

microbial reassembly in degraded tropical systems. By identifying taxonomic and network-based indicators of microbial reorganization, this study advances our understanding of community assembly theory and offers guidance for restoration practices in post-agricultural landscapes.

1. Introduction

Soil microbiomes are central to ecosystem function, regulating essential processes such as nutrient cycling, organic matter dynamics, and plant community composition (Van Der Heijden et al., 2008), as well as directly impacting plant responses to climate change and stress (Zahn and Amend, 2019; Silverstein et al., 2023). Land-use conversion from biodiverse ecosystems to intensive agricultural monocultures significantly alters microbial community structure and disrupts microbial networks, with lasting negative impacts on soil health, resilience, and ecosystem stability (Tsiafouli et al., 2015; Peng et al., 2024). As global restoration efforts intensify, understanding microbial community assembly following disturbance is increasingly critical for predicting ecosystem recovery and guiding effective management strategies.

This assembly trajectory is governed by multiple ecological processes including dispersal, environmental selection, drift, and historical contingency (Fukami, 2015; Wainwright et al., 2020; Mazzella et al., 2025). Additionally, community coalescence, the merging of previously distinct microbial communities, further complicates restoration trajectories by creating novel species interactions and assembly patterns (Rillig et al., 2015). Despite advances in community assembly theory, critical questions remain: Do bacterial and fungal communities show similar successional dynamics? How does soil chemistry mediate these trajectories? To what extent are microbial recovery patterns observed in temperate systems broadly applicable to tropical environments?

Empirical studies have provided conflicting evidence regarding bacterial and fungal recovery pathways. For instance, research in high-elevation grasslands indicates bacterial communities recover more rapidly than fungal communities following restoration (Du et al., 2025). Conversely, studies of drought-stressed soils (De Vries et al., 2018) and reclaimed mining lands (Sun et al., 2017) report variable and sometimes opposing patterns. Some work indicates that bacterial and fungal communities are often decoupled with respect to environmental drivers of alpha diversity (Shen et al., 2020a, 2020b; Liu et al., 2020), although these broad-scale measures alone may fail to fully capture changes relevant to ecosystem function and restoration trajectories. For example, shifts in bacterial and fungal community composition during tropical forest succession vary significantly across precipitation regimes even when alpha diversity remains static (Saltonstall et al., 2025). Given this variability, it is essential that microbial succession studies integrate both taxonomic Kingdoms (Jiao et al., 2022) along with comprehensive soil chemistry measurements that may differentially mediate bacterial and fungal responses (Jiang et al., 2021). Integrating sensitive metrics such as cross-domain interactions and keystone taxa identification may provide deeper insights into microbial community recovery and resilience (Banerjee et al., 2018; Wagg et al., 2019).

Rewilding initiatives, which restore intensively managed landscapes to more biodiverse states, offer invaluable opportunities to study microbial succession, community coalescence, and network resilience under real applied scenarios (Mittelman et al., 2022). Microbial responses to rewilding are shaped by a complex interplay of ecological filters (e.g., dispersal limitation, environmental selection), legacy effects of past land use (Dang et al., 2024), recolonization by plants and faunal communities (Van Der Putten et al., 2013), and stochastic processes (Dong et al., 2021; Liu et al., 2021). Key questions remain regarding the predictability of microbial reassembly during restoration. Additionally, the degree to which the patterns and processes observed in better-studied temperate agricultural systems are applicable more broadly remains unknown. How they apply in tropical systems is an especially significant knowledge gap.

Tropical oil palm plantations represent an ideal system for investigating microbial community assembly and ecological restoration. The conversion of tropical forests to oil palm agriculture is a primary driver of deforestation, dramatically altering biodiversity, soil chemistry, and ecosystem functioning (Turner et al., 2008; Lim et al., 2024). Intensive oil palm cultivation practices simplify microbial community structure, reduce beneficial mutualist taxa, and create persistent legacy effects that constrain restoration potential (Ahmad Ali et al., 2012; Guillaume et al., 2016). The distinct and intensive disturbance regime associated with palm oil cultivation provides a valuable context to study microbial succession, community coalescence, and ecosystem resilience under realistic ecological scenarios of global importance.

In this study, we leveraged a five-year rewilding chronosequence in tropical soils spanning actively managed oil palm plantations through various stages of rewilding to explicitly track bacterial and fungal community recovery. By integrating high-resolution amplicon sequencing, ecological network analyses, and statistical modeling, we offer a comprehensive assessment of microbial recovery and resilience following tropical agricultural rewilding. Using paired full-length 16S/ITS metabarcode sequencing, we combined detailed community composition assessments (alpha and beta diversity), soil chemical analyses, ecological network modeling, differential abundance analyses, and machine learning methods to examine microbial community assembly. Specifically, we hypothesize that: 1) bacterial and fungal communities will follow distinct successional trajectories; 2) soil chemistry will mediate microbial recovery; and 3) we aim to determine whether microbial networks regain complexity and resilience or remain constrained by past land use. Addressing these questions can advance microbial assembly theory and inform practical restoration strategies.

2. Methods

2.1. Site description and soil sampling

Samples were collected in January 2024 from land owned by "A Little Wild" in the Malaysian state of Johor (https://alittlewild.com/). Five 50 m × 20 m plots were selected along a rewilding chronosequence (SI Fig. 1). Plot 1 contained actively growing oil palm trees. In plot 2, oil palms had been cut but left in place and the plot left fallow for one year. Plot 3 was in the initial stage of rewilding and had recently been planted with native vegetation. Plot 4 was two years into rewilding, and plot 5 had undergone rewilding for three years. All plots were planted with native vegetation only. From each plot, 16 randomly located soil samples were collected to a depth of approximately 5 cm below the surface, prior to collection any surface litter was removed. Each sample (30–40 g) was collected in sterile 50 mL Falcon tubes. Samples were kept on ice and transferred to −80 °C storage within six hours of collection.

2.2. DNA extraction and library preparation

Prior to DNA extraction, all samples were homogenized. DNA was then extracted from 250 mg of collected sample using the Qiagen DNeasy PowerSoil Kit following the manufacturer's protocol. Bead beating was performed in Qiagen 2 mL tubes for three 1-min cycles at 6 m/s using an Omni Bead Ruptor Elite, with a 5-min rest between cycles. All steps were conducted in a biological safety cabinet that had been decontaminated with 10 % bleach, 70 % ethanol, and UV-sterilized for 20 min.

Extracted DNA was submitted to Novogene (Singapore) for amplification, library preparation, and sequencing. Bacterial 16S rRNA genes

(V1–V9 region) were amplified using primers 27F (5'-AGRGTTYGA-TYMTGGCTCAG-3') and 1541R (5'-RGYTACCTTGTTACGACTT-3') (Frank et al., 2008). Fungal ITS1–5.8S-ITS2 regions were amplified using primers ITS9MUNngs (5'-TACACACCGCCCGTCG-3') and ITS4ng-sUni (5'-CCTSCSCTTANTDATATGC-3') (Tedersoo and Anslan, 2019). Libraries were prepared using PacBio Kinnex protocols and sequenced on the PacBio Revio platform. Bacterial and fungal libraries were sequenced separately. Negative controls (PCR blanks and extraction blanks) and mock communities (ZymoBiomics D6300) were processed in parallel for quality control.

2.3. Bioinformatics and sequence processing

Raw sequences were processed in R using a custom pipeline (Zahn and Hjelmen, 2025). Primer trimming was performed using *cutadapt* (v. 3.5) (Martin, 2011). Sequences were quality-filtered and denoised using *DADA2* (v. 1.31.0) (maxEE = 2, truncQ = 2, maxN = 0) (Callahan et al., 2016), followed by chimera removal and Amplicon Sequence Variant (ASV) inference.

Contaminants were identified with the prevalence method in *decontam* (v. 1.24.0) (Davis et al., 2018) using negative control samples, probable contaminant ASVs were then removed from all samples. ASVs with fewer than 100 reads were discarded. Remaining reads averaged 69,526 (bacteria) and 30,606 (fungi) per sample (See S.I. Table 1). Taxonomic assignments were made using SILVA (v. 138.1) for bacteria (Quast et al., 2013) and Eukaryome Longread (v. 1.9) for fungi (Tedersoo et al., 2024) with 80 % minimum bootstrap confidence. A total of 11,509 bacterial and 687 fungal high-quality ASVs were retained. Assigned taxonomic names were standardized using the *bac-dive* (v. 0.8.0) (Goeker, 2022) and *mycobank* (v. 0.1.0) (Zahn, 2024a) R packages. Sequences were aligned with *DECIPHER* (v. 3.0.0) (Wright, 2016) and phylogenies inferred with neighbor-joining tree using Jukes-Cantor distance in *phangorn* (v. 2.11.1) (Schliep, 2011). Ambiguous placements were resolved with reference backbone trees (Li et al., 2021; McDonald et al., 2024). Phylogenetic trees were incorporated into *phyloseq* (v. 1.48.0) (McMurdie and Holmes, 2013) objects for downstream analysis. ASVs were collapsed to the species level for parallel diversity analyses. The pipeline, including scripts to download raw data, is available as an archived GitHub release (Zahn and Hjelmen, 2025). Raw sequence data are deposited in the SRA under accession PRJNA1117193.

2.4. Soil chemistry analyses

Samples were dried at 50 °C until a constant mass was achieved, ground with a mortar and pestle, and sieved to 2 mm. Total nitrogen, phosphorus, hydrogen, and carbon content (%) were measured with a CHNS Elemental Analyzer (Thermo Fisher Scientific, Waltham, MA). Phosphorus (ppm) was measured via ICP-OES (Perkin Elmer, Waltham, MA). pH was measured on non-dried samples using a 1:2.5 soil:water slurry with a Mettler Toledo pH electrode.

2.5. Statistical analyses

All statistical analyses were performed in R (v. 4.5.0) (R Core Team, 2024). Soil variables were modeled using one-way ANOVA with "rewilding stage" as a predictor, followed by Tukey HSD tests. Linear mixed-effects models were fitted using *lmerTest* (v. 3.1.3) (Kuznetsova et al., 2017) with fungal ASV richness as the response, plot as a random effect, and five scaled soil variables (pH, carbon, hydrogen, nitrogen, and phosphorus content) as fixed effects. All predictors were z-transformed to allow direct comparison of effect sizes within a single model. Assumptions of normality and homogeneity of variance were assessed via residual diagnostic plots, which indicated no major violations.

Community composition was analyzed with NMDS ordinations, PERMANOVA, and beta dispersion metrics using Unifrac distances

(Lozupone et al., 2011) at the ASV and species levels via *vegan* (v. 2.6.6.1) (Oksanen et al., 2025). Ordinations were performed using non-metric multidimensional scaling (NMDS) via the ordinate () function in *phyloseq*, based on unweighted UniFrac distances calculated from within-sample relative abundances. NMDS was run in two dimensions (k = 2), yielding stress values of 0.17 for fungi and 0.10 for bacteria. Sample-wise beta dispersion values, calculated as distances to group centroids, were analyzed separately for bacteria and fungi using generalized linear models with rewilding stage as a predictor to assess trends in community heterogeneity.

To identify which soil properties were most strongly associated with microbial community composition, we fitted soil chemistry variables onto the NMDS ordinations using the **envfit** function in *vegan* (9999 permutations). Prior to analysis, all environmental variables were centered and scaled (z-scored) to account for differences in measurement units. The squared correlation coefficient (r^2) and false-discovery-rate-adjusted (Benjamini-Hochberg correction) q values were used to assess the strength and significance of each variable's alignment with the ordination. Variables with $q < 0.05$ were considered significant. Because the small variance in NMDS axis scores produced disproportionate arrow scaling, environmental vectors were not plotted.

Generalized dissimilarity models were implemented using the gdm package (v. 1.5.0.9.1) (Fitzpatrick et al., 2022) to quantify the influence of soil chemistry and geographic distance on bacterial and fungal community turnover. Separate models were constructed for each domain using relative abundance data. Predictors included all soil chemistry variables and geographic distance derived from sample coordinates. Nonlinear contributions of each variable were interpreted from I-spline transformations. Compositional variability was assessed using the phylogenetically weighted Framework for Analyzing Variability in Assemblages (FAVA) (Morrison et al., 2025) with 1000 bootstraps to measure the temporal stability of bacterial and fungal community structures.

Microbial co-occurrence networks were inferred using the *SpiecEasi* package (v. 1.1.3) (Kurtz et al., 2024) with Meinshausen-Bühlmann neighborhood selection and stability selection. PermANOVA showed that rewilding stage was a strong predictor of community structure, so replicates were pooled by domain/stage for network inference to reduce site-specific biases (Du et al., 2025). Separate networks were constructed for fungi, bacteria, and combined communities within each rewilding stage (five stages total). All networks were based on species-level taxonomic aggregations and constructed from centered log-ratio transformed relative abundance data. Phylogenetic trees were removed prior to merging datasets. No explicit abundance or prevalence filtering was applied before network inference. Full networks for each domain were converted to *igraph* objects (v. 2.0.3) (Csárdi et al., 2023), and per-sample induced subgraphs were extracted by identifying taxa present in each sample and subsetting the corresponding vertices in the global network.

A suite of graph-theoretic metrics (including degree distribution, mean distance, betweenness, closeness, coreness, clustering coefficient, clique number, number of vertices, and global efficiency) was computed for each sample's subgraph to quantify local network structure. Degree and coreness capture how well-connected individual taxa are within the network, reflecting potential generalist or hub behavior. Mean distance and global efficiency describe how easily interactions or resources could move through the community, with higher efficiency indicating a more integrated network. Betweenness and closeness quantify the centrality of taxa within interaction pathways, highlighting species that may mediate cross-lineage or cross-functional connections. Clustering coefficient and clique number measure local cohesion among neighboring taxa, often interpreted as ecological modularity or guild formation. The number of vertices represents the taxonomic richness of the active interaction network. These metrics were then related to observed species richness using linear mixed-effects models with richness as the response variable, network attributes as scaled fixed effects, and rewilding stage

as a random intercept. Differences in network topology across rewilding stages were further assessed using ANOVA on scaled network metrics and visualized with boxplots and smoothed scatterplots.

Hub taxa were identified using the HITS algorithm (Kleinberg, 1999) implemented in the *hubfindr* package (v. 0.1.0) (Zahn, 2024b). Separate analyses were performed on fungal, bacterial, and combined domain-level networks. Within each global network, nodes with hub scores greater than one standard deviation above the mean were designated as hubs. To identify potential keystone taxa, sample-specific subgraphs were also extracted, and hub scores were recalculated at the sample level. Taxonomic identities of hub taxa were assigned based on species-level annotations from the corresponding phyloseq objects.

Beta-binomial models using *corncob* (v. 0.4.1) (Martin et al., 2022) identified differentially abundant taxa between rewilding stages, applying an FDR-adjusted P value cutoff of 0.05 (Benjamini-Hochberg method). Abundance was modeled as a function of rewilding stage, with dispersion held constant across groups. Wald tests were used to compare each taxon against a null model with no stage effect.

Random forest models were trained using the *ranger* package (v. 0.16.0) (Wright and Ziegler, 2017) to identify taxa most important for distinguishing rewilding stages. Models were fit separately for fungi and bacteria using 999 permutations, and taxon-level variable importance scores based on permutation importance were extracted using the *vip* package (v. 0.4.1) (Greenwell and Boehmke, 2020). Taxa were classified as discriminatory if their importance scores fell within the top (fourth) quartile of all taxa within their respective model.

Taxa were classified as ecologically important if they met all three independent criteria: (1) significantly differentially abundant across rewilding stages based on beta-binomial models (*corncob*, FDR < 0.05), (2) identified as network hubs with hub scores exceeding one standard deviation above the mean (*hubfindr*), and (3) ranked in the top quartile of random forest variable importance scores (*ranger* + *vip*). This approach ensured that selected taxa were not only statistically responsive to rewilding but also structurally central in microbial networks and highly predictive of ecological state. All models were applied to unrarefied, compositional data; CLR transformation was used to account for compositionality in network inference. ASVs were merged at the species level for final reporting.

3. Results

3.1. Soil chemistry shifts dramatically after two years of rewilding

Soil chemistry changed significantly over the five-year rewilding period, with notable increases in pH, carbon (C), nitrogen (N), and phosphorus (P) as restoration progressed (Fig. 1, SI Table 2). The most pronounced changes occurred after the second year of restoration, highlighting a potential threshold beyond which soil microbial and biogeochemical processes drive more substantial improvements in soil function. Mixed-effect models indicated that microbial alpha diversity was significantly associated with various soil chemistry properties. Bacterial species richness was significantly linked to increased pH (lmer: $P = 0.01$; r2 = 0.30) while fungal richness was linked to both pH (lmer: $P < 0.0005$; r2 = 0.37) and carbon (lmer: $P = 0.048$; r2 = 0.37; SI Fig. 2, SI Table 3).

3.2. Communities transition from disturbed to mature assemblages during rewilding

Bacterial community composition changed notably throughout the five-year rewilding process (Fig. 2A). Proteobacteria and Acidobacteriota remained dominant across all treatments, but their relative abundances fluctuated over time. Proteobacteria, which were highly abundant in oil palm soils, gradually decreased in relative abundance during restoration, while Acidobacteriota and Actinobacteriota became more prominent in later restoration stages.

Other phyla, such as Bacteroidota and Cyanobacteria, showed increases in relative abundance, particularly after the second year of restoration. These groups are often associated with organic matter decomposition and nitrogen cycling (Chen et al., 2022; Huang et al., 2023), suggesting a transition toward a more functionally diverse and resilient soil microbial community. Firmicutes and Planctomycetota, which were relatively abundant in early restoration stages, declined in later years, indicating a shift from disturbance-adapted taxa to those associated with more stable, nutrient-cycling ecosystems.

Overall, the observed trends suggest that bacterial communities were transitioning from those adapted to high-input, disturbed agricultural conditions toward microbial assemblages characteristic of more natural, self-sustaining ecosystems. These shifts likely play a crucial role in regulating soil chemistry changes, particularly in carbon and nitrogen cycling, during rewilding.

Fungal community composition shifted over the five-year rewilding period, with notable changes in the relative abundances of major fungal phyla (Fig. 2B). Across all treatments, Ascomycota was the dominant fungal phylum, and its relative abundance increased over time, while Basidiomycota relative abundance decreased as restoration progressed. Early rewilding stages (<1 year) showed a relatively high proportion of Rozellomycota and Mucoromycota, but these phyla declined in later years.

By the 3–4 year stage, fungal communities had diversified, with an increase in Basidiomycota and minor contributions from Glomeromycota and Chytridiomycota. These shifts suggest a transition from fungal communities adapted to disturbed agricultural soils toward those associated with more natural, functionally diverse ecosystems. The increase in Basidiomycota may reflect enhanced decomposition and organic matter cycling, which aligns with observed increases in soil carbon and nitrogen content.

3.3. Fungal and bacterial richness increase steadily across rewilding stages

Fungal richness increased significantly across rewilding stages (Fig. 3). The lowest values were in oil palm soils, and richness increased steadily through the 3–4 year stage. The observed increase in fungal diversity aligns with the transition from disturbance-adapted taxa (e.g., fast-growing opportunists) toward more diverse, functionally complex fungal assemblages. This trend suggests that fungal community succession follows a trajectory where decomposer and symbiotic taxa become more dominant as organic matter accumulates and soil chemistry stabilizes.

Bacterial richness also increased significantly over the rewilding period, though with less variability than fungi (Fig. 3). The lowest richness was observed in oil palm soils, while the highest diversity was found in the 3–4 year restoration stage. This suggests that as restoration progresses, bacterial communities become more diverse, likely due to increased habitat heterogeneity, organic matter accumulation, and stabilized nutrient cycling. The sharp increase in diversity during the <1 year transition may reflect an initial microbial colonization event following reduced agricultural inputs, with a more gradual increase in subsequent years.

3.4. Microbial community structure diverges over time, with fungi showing greater variability

Bacterial communities underwent significant compositional changes as rewilding progressed (Fig. 4A). The increasing separation of clusters over time indicates that bacterial communities became more differentiated from the original oil palm state, likely due to the observed changes in soil chemistry and organic matter accumulation. Fungal communities shifted early in the rewilding process, with later stages continuing to differentiate (Fig. 4B). The greater dispersion in fungal communities suggests that fungi respond more variably to rewilding compared to
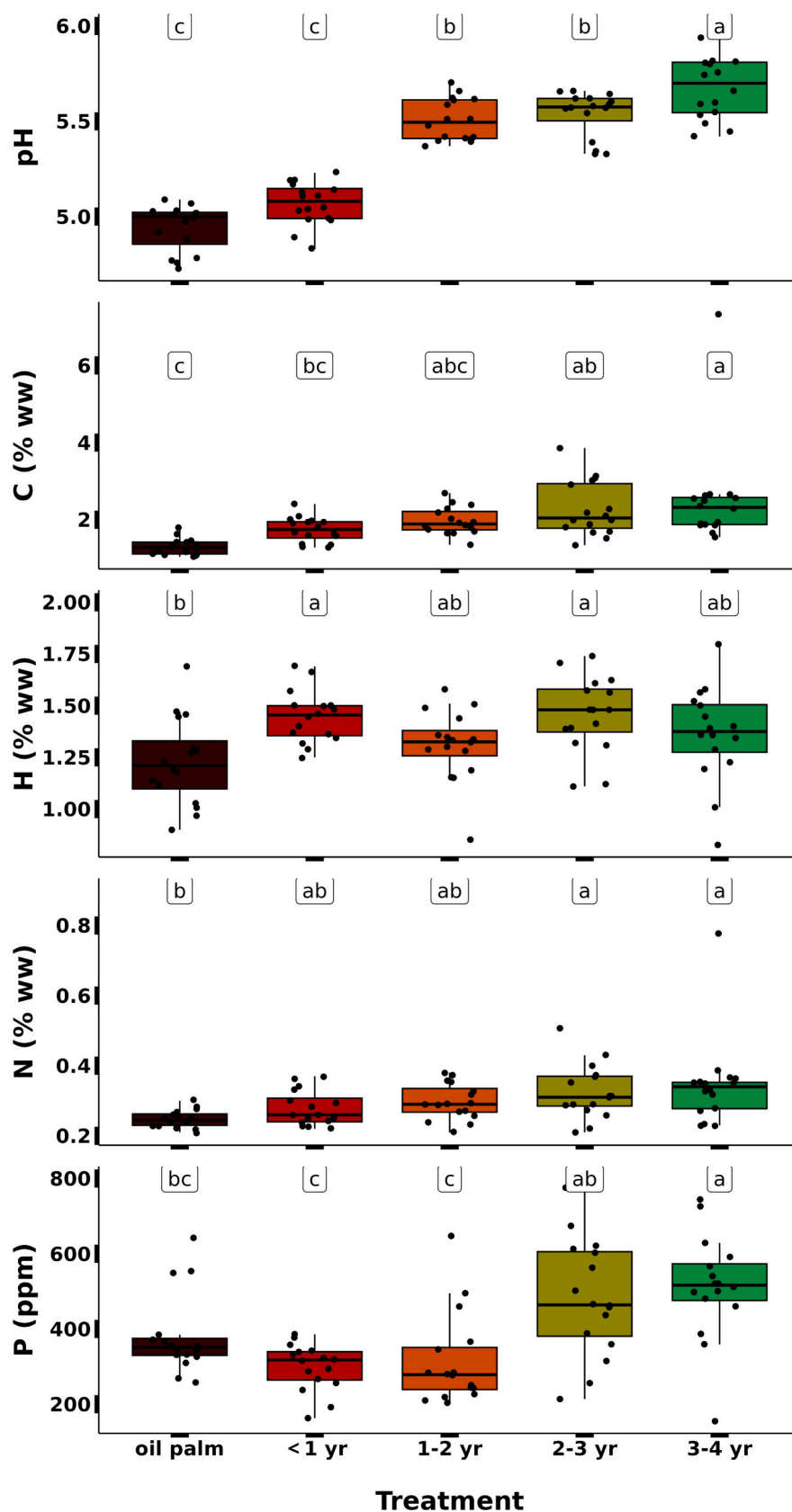
Fig. 1. Changes in soil chemistry across rewilding stages. Boxplots show soil pH and concentrations of carbon (C), hydrogen (H), nitrogen (N), and phosphorus (P) across the rewilding chronosequence. Letters above boxes indicate groups that differ significantly based on Tukey HSD post hoc tests following one-way ANOVA ($p < 0.05$).
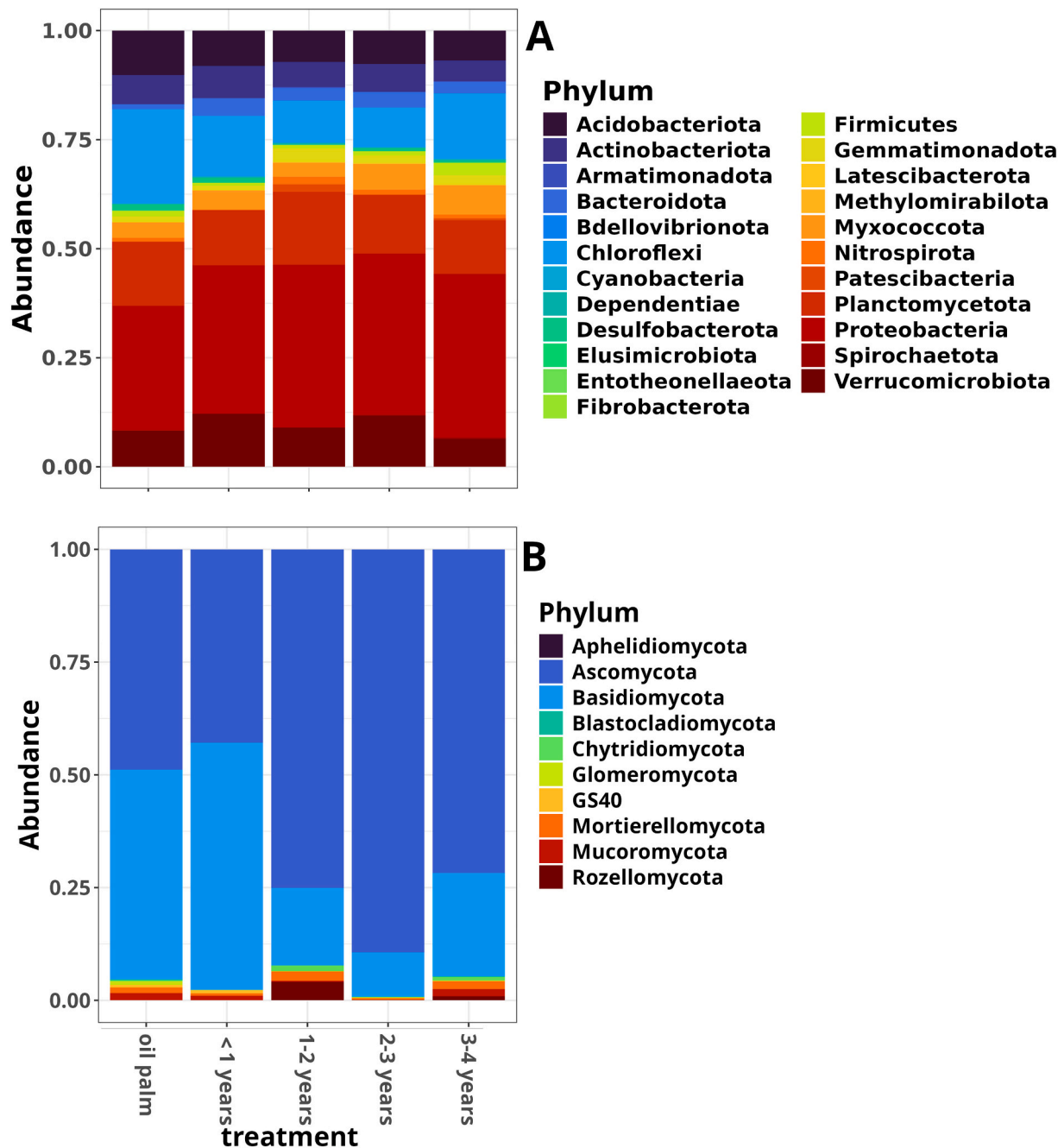
Fig. 2. Relative phylum-level composition of bacterial (A) and fungal (B) communities across rewilding stages. Bars represent the mean relative abundance of each phylum pooled across replicates within a stage.

bacteria, possibly due to differences in substrate availability, plant-fungal interactions, and soil structure changes.

Fungal beta-dispersion was highest in oil palm soils, indicating a more heterogeneous fungal community structure under industrial agriculture. As rewilding progressed, fungal beta-dispersion decreased, particularly after the <1 year transition (Fig. 4C). This suggests that fungal communities were less stable and more stochastic, possibly due to inconsistent resource availability, agrochemical use, or other soil disturbances. Over time, fungal communities become more stable and predictable as restoration progresses, likely due to increasing organic matter accumulation and reduced disturbance. Unlike fungi, bacterial beta-dispersion was consistently low across all stages (Fig. 4C), indicating that bacterial communities were more uniform within each treatment and experienced a more gradual compositional shift rather

than highly variable community assembly.

Partial community dissimilarity metrics showed differences in the way geographic distance and soil chemistry affected bacterial and fungal community structure (Fig. 5). Fungal communities showed a stronger spatial structure than bacterial communities, though the effects of distance were attenuated at around 100 m for both groups. This suggests that fungal dispersal was more limited by geographic distance, likely due to differences in propagule movement, dependence on plant hosts, or stochastic colonization dynamics. Both bacterial and fungal richness increase with pH, though bacteria show a slightly steeper response.

Fungal communities showed a much stronger response to carbon availability than bacteria, suggesting that fungal richness is highly dependent on organic matter accumulation. However, the effect of C on fungal community structure leveled off at around 3 % ww. Bacterial
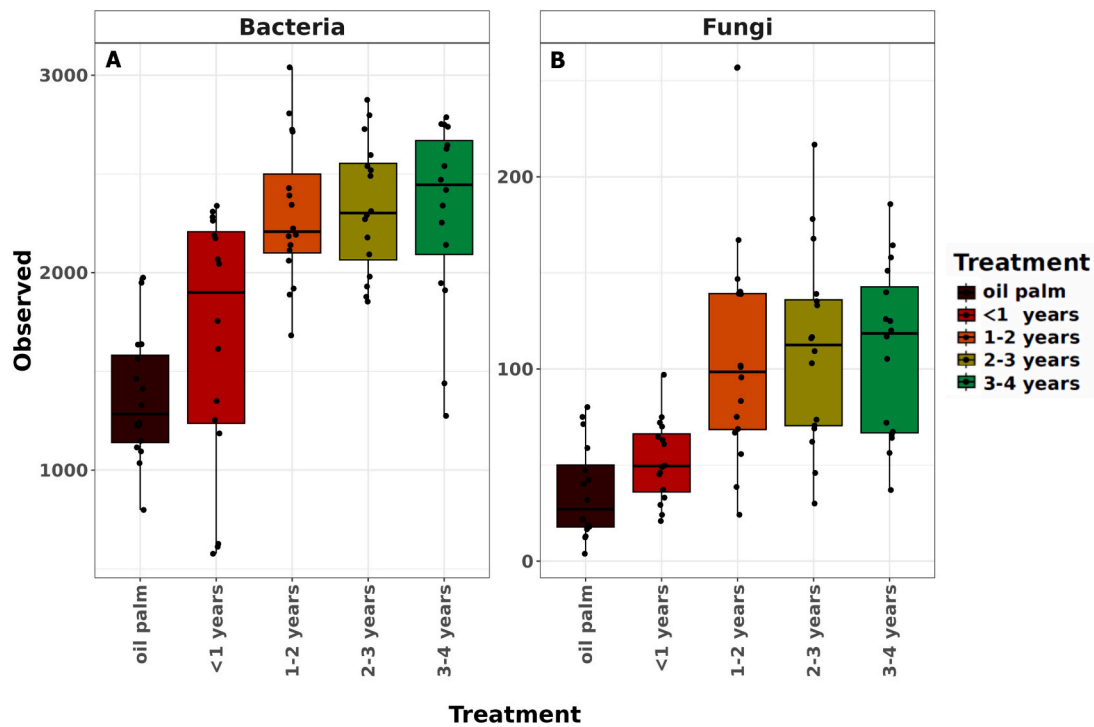
Fig. 3. Changes in bacterial and fungal species richness across rewilding stages. Boxplots show observed amplicon sequence variant (ASV) richness for bacterial (A) and fungal (B) communities across treatments along the rewilding chronosequence.

richness also increased with carbon but at a slower rate, indicating that while bacteria contribute to organic matter decomposition, their diversity was less directly tied to carbon pools.

Fungal richness increased steadily with hydrogen content, while bacterial richness remained relatively unaffected. This may indicate that fungal metabolic activity is more strongly tied to hydrogen levels in soil organic matter. Bacterial richness showed a strong positive correlation with nitrogen content, leveling off at around 0.4 % ww, while fungi showed almost no response. Both bacterial and fungal richness steadily increased with phosphorus, but bacteria show a slightly stronger response at higher phosphorus levels.

Envfit analysis showed that for fungi, pH had strongest correlation with the NMDS configuration (r^2 = 0.72, q = 0.0005), followed by carbon (r^2 = 0.17, q = 0.0045), phosphorus (r^2 = 0.14, q = 0.0045), and nitrogen (r^2 = 0.10, q = 0.023). Hydrogen content was not significant (q > 0.05). Similarly, for bacteria, pH was the dominant correlate (r^2 = 0.67, q = 0.0005), followed by carbon (r^2 = 0.15, q = 0.0025), phosphorus (r^2 = 0.13, q = 0.008), and nitrogen (r^2 = 0.10, q = 0.018). Hydrogen again showed no significant association (q > 0.05).

FAVA values, which reflect similarities in the spatial or temporal dynamics shaping variability, were calculated for bacteria and fungi separately at each rewilding stage to allow for the incorporation of taxon abundances. FAVA pairwise comparisons showed significant differences in compositional similarity congruent with PermANOVA test results (SI Fig. 3). Oil palm and the <1 year stage had similar compositionality in both bacterial and fungal communities, but this diverged and later stages all grouped together.

3.5. Distinct bacterial and fungal taxa consistently track rewilding progress

A subset of bacterial (N = 9) and fungal (N = 32) taxa were identified as ecologically important by all three of our approaches (differential abundance via *corncob*, variable importance scores within the fourth quartile in random forest models, and hub scores one standard deviation above the mean) and showed distinct shifts in mean relative abundance

across rewilding stages (Fig. 6). In bacterial communities, five dominant classes (Alphaproteobacteria, Bacilli, Blastocatellia, Gammaproteobacteria, and Polyangia) increased in relative abundance over time, with Alphaproteobacteria and Polyangia consistently accounting for the largest proportions, particularly in the later rewilding stages. Fungal communities exhibited greater compositional turnover, with Sordariomycetes increasing sharply from the <1 year stage onward and dominating the community after. Other fungal classes such as Dothideomycetes and Tremellomycetes were more prevalent in oil palm soils but declined or fluctuated during the rewilding process. These key microbial taxa linked to centrality and predictive importance are not static, but rather they display domain-specific and time-structured dynamics as rewilding progressed.

3.6. Microbial networks become more connected and complex over time

In bacterial networks, global efficiency, max degree, mean betweenness, and number of vertices (nodes) increased as rewilding progressed, showing that bacterial networks became more connected and integrated, with more interactions forming between taxa over time since rewilding (Fig. 7A). The <1 year stage exhibited an increase in network connectivity compared to oil palm but remained lower than later stages, suggesting a transitional microbial community in which bacterial interactions are still reassembling. Oil palm soils have lower values for clustering coefficient, betweenness centrality, and number of vertices, indicating a more fragmented bacterial network with weaker interactions, possibly due to high disturbance and reduced microbial diversity under monoculture conditions.

Unlike bacteria, fungal networks showed greater fluctuations in connectivity metrics across time (Fig. 7B). The clustering coefficient is highest at <1 year, then decreases slightly in later stages, indicating that fungal communities initially establish tightly connected subnetworks before diversifying. The number of vertices and mean betweenness increased across rewilding stages, indicating that more fungal taxa are interacting as soil rewilding progresses. The mean closeness and centrality remained relatively stable, suggesting that the overall efficiency
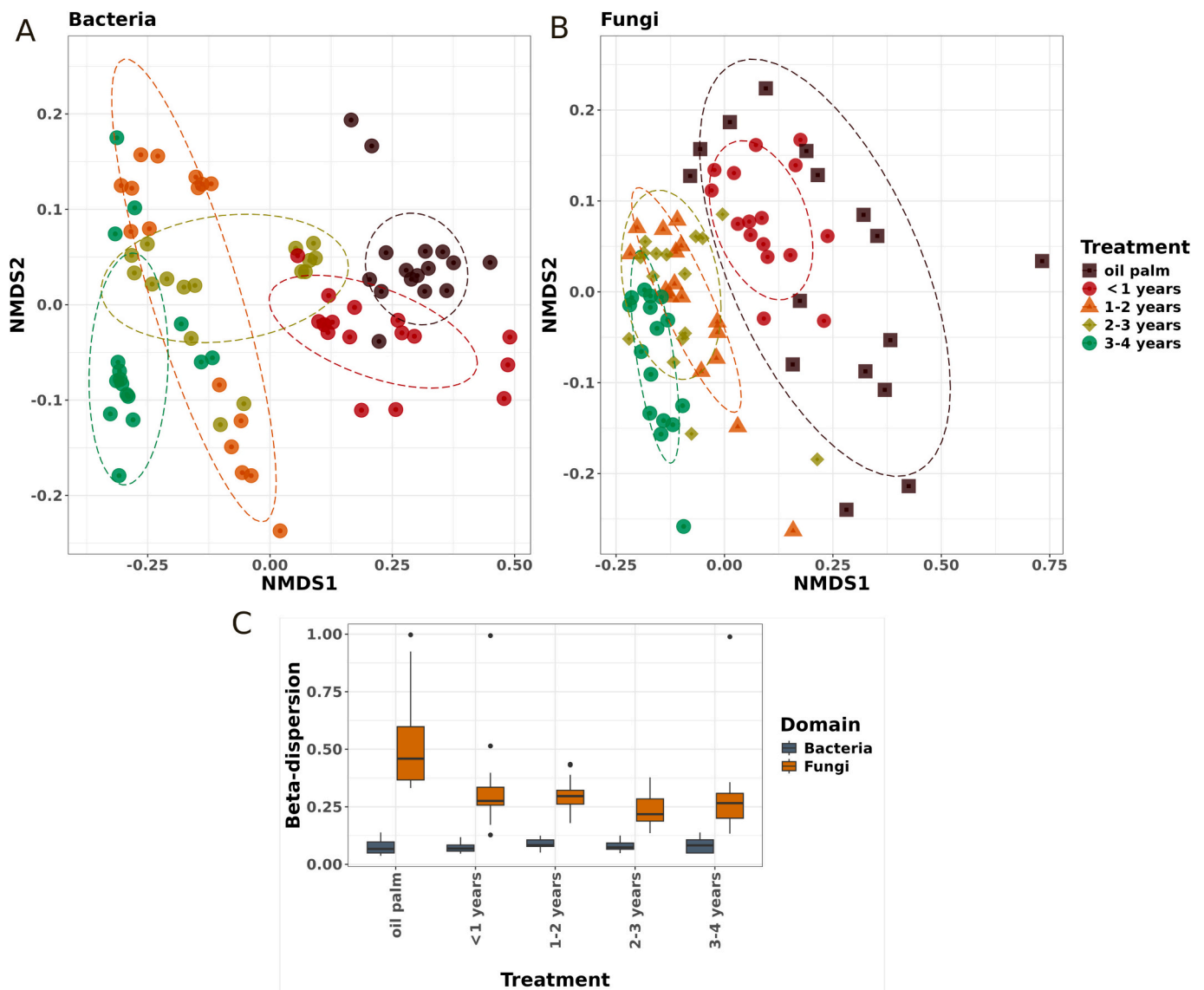
Fig. 4. NMDS plots showing bacteria (panel A) and fungi (panel B) community dissimilarity. Ellipses represent the 95 % confidence intervals around grouped centroids. Panel C shows beta-dispersion boxplots across rewilding stages for bacteria (gray) and fungi (orange). Fungal communities are more heterogeneous than bacteria across all rewilding stages, but show increasing homogenization over time.

of information flow in fungal networks does not shift as dramatically as in bacteria. Oil palm fungal networks had the lowest betweenness centrality and number of vertices, suggesting that fungal interactions were limited under intensive agriculture.

In combined networks with both bacterial and fungal interactions, the number of vertices, mean betweenness, and max degree all increased over time, reinforcing the trend that microbial networks become more interconnected as rewilding progresses (Fig. 7C). The increase in mean degree suggests that taxa form more interactions over time, potentially due to the recovery of symbiotic and decomposer relationships. By 3–4 years, network complexity was at its highest, indicating that microbial community interactions are stabilizing into a mature, functionally connected community.

Networks in oil palm soils tended to be more fragmented, with weak interactions and low microbial connectivity. Early rewilding stages showed rapid network restructuring, particularly in fungal communities, which initially formed tight clusters before stabilizing. Later rewilding stages had highly connected microbial networks, suggesting that functional relationships between microbes increased with soil recovery. Bacteria and fungi followed different trajectories, with bacteria

showing more linear increases in complexity, while fungal networks fluctuated before stabilizing. Together, these results highlight that rewilding promotes microbial connectivity for fungi and bacteria, but that they follow divergent trajectories. Complete network plots for each group and rewilding stage are available in the Supporting Material (SI Fig. 4).

3.7. Rewilding restructures community assembly

Across the rewilding chronosequence, bacterial community composition shifted markedly in both richness and relative abundance at the order level (Fig. 8A). Early-stage soils (<1 year) contained a relatively limited subset of bacterial orders, reflecting a simplified community structure consistent with oil palm monoculture. As rewilding progressed, the number of unique ASVs per order increased substantially, with a broader distribution across phylogenetically diverse lineages. Orders such as Chitonophagales, Pirellulales, and Burkholderiales showed an increase in unique ASVs and relative abundance across time, suggesting that rewilding fosters recruitment of taxa commonly associated with nitrogen mineralization activity and complex aromatic
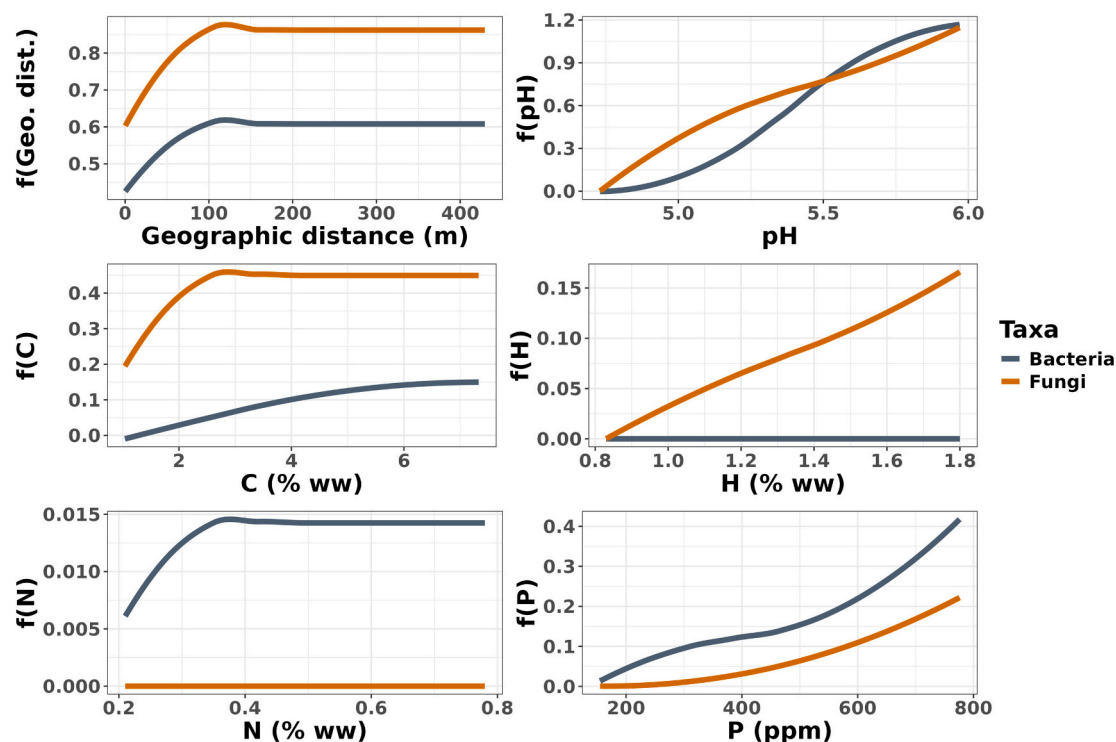
Fig. 5. Partial community distance plots (GDM) showing the isolated effects of geographic distance and soil chemistry components on bacterial (gray) and fungal (orange) community structure. X-axes show the gradient of each variable present in the full data set. Y-axes show the magnitude of community turnover.
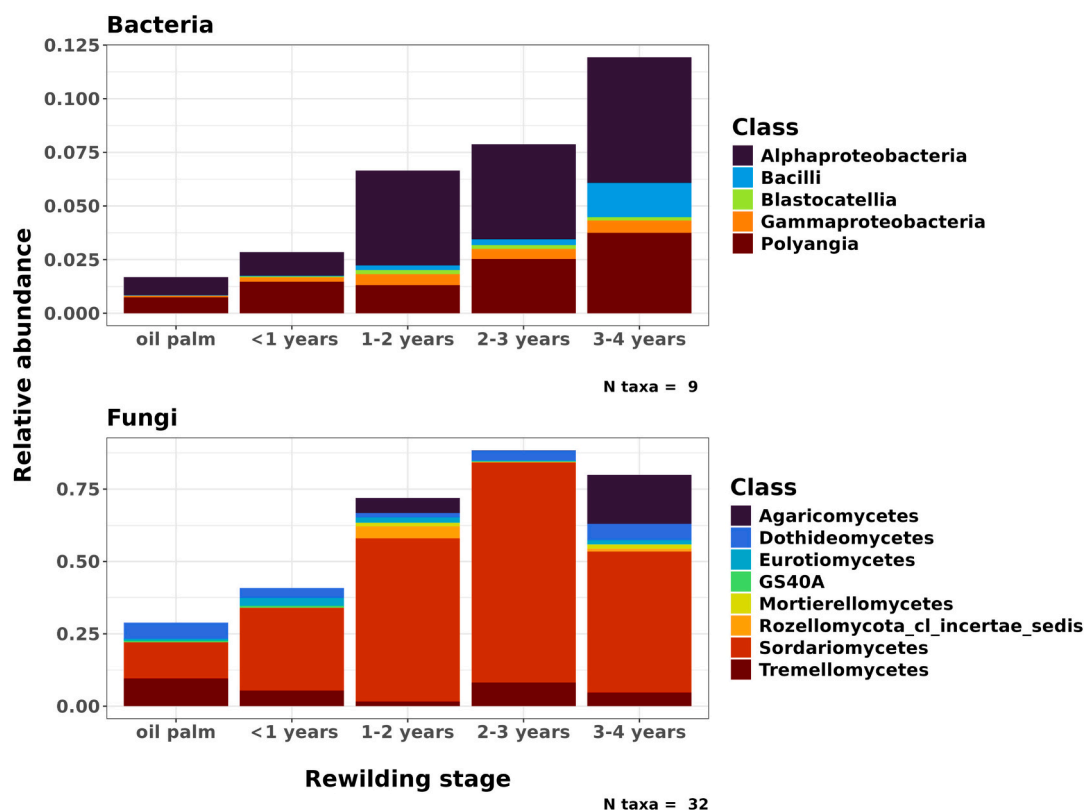

Fig. 6. Mean relative abundances of key bacterial (top panel) and fungal (bottom panel) taxa across rewilding stages. These taxa were identified by *corncob* as having significantly differential abundance between rewilding stages, by random forest models as having variable importance scores within the fourth quartile, and by *hubfindr* as having hub scores greater than one standard deviation above the mean. Taxa are presented grouped by Class.
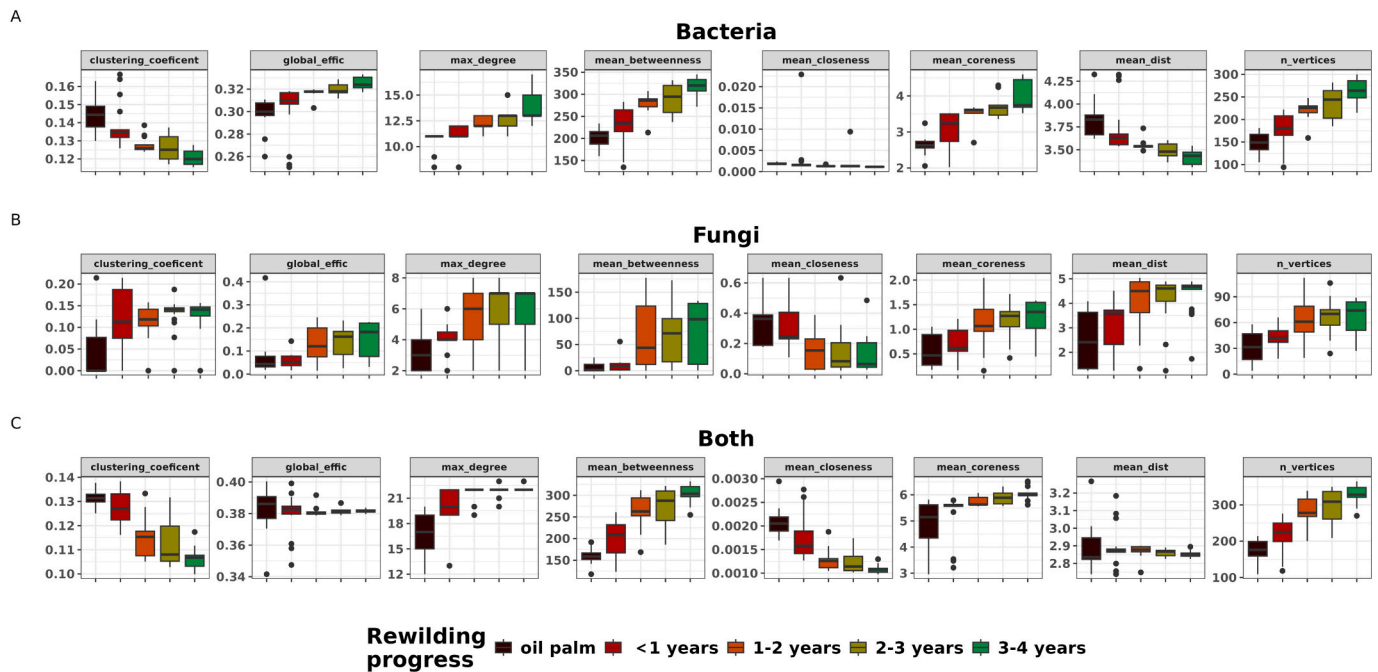
Fig. 7. Changes in microbial network topology across rewilding stages for bacterial (top panel), fungal (middle panel), and combined cross-domain (bottom panel) networks. Boxplots show variation in metrics describing local and global network structure, including clustering coefficient, global efficiency, maximum degree, betweenness, closeness, coreness, mean path distance, and number of vertices (nodes).

degradation.

Fungal community composition also shifted markedly across rewilding stages, with certain orders showing steep increases in both ASV richness and relative abundance (Fig. 8B). Notably, Glomerales and Agaricales expanded significantly in later-stage rewilded plots, consistent with enhanced mycorrhizal associations and saprotrophic turnover. Meanwhile, orders such as Tremellales and Saccharomycetales showed stable ASV counts and relative abundance, suggesting a decline in the importance of fast-growing, disturbance-adapted taxa. Late-stage additions of taxa such as Spizellomycetales and Venturiales, which have many parasitic member taxa (Paulitz and Menge, 1984; Shen et al., 2020b), point to increasing nice diversity across rewilding stages. The taxonomic turnover of fungi was phylogenetically broad, reflecting a dynamic reorganization of fungal niches as plant communities and soil chemistry evolved during rewilding.

4. Discussion

4.1. Soil chemical changes reflect early-stage nutrient accumulation

Our findings indicate that several soil chemical properties shift rapidly following the cessation of oil palm cultivation and the onset of rewilding. Total carbon, nitrogen, and phosphorus content showed significant increases between the oil palm and rewilded plots, with a clear positive trajectory over time. These patterns suggest that plant inputs and microbial turnover associated with early rewilding efforts may rapidly enhance soil fertility. Notably, C:N ratios declined slightly over time, potentially indicating improved nitrogen availability relative to carbon inputs. Such trends are consistent with studies showing nutrient pool accumulation within the first few years of restoration (Hernández et al., 2013; Wei et al., 2023). These chemical shifts were strongly predictive of microbial community composition in our generalized dissimilarity models, reinforcing the central role of nutrient dynamics in structuring post-agricultural microbial communities.

4.2. Bacterial and fungal diversity increase with rewilding, but along distinct trajectories

Alpha diversity analyses revealed a significant increase in bacterial richness across the rewilding gradient, with richness levels rising steadily from oil palm to the 3-year rewilded plots. Fungal richness also increased but plateaued more quickly, showing smaller differences between mid- and late-stage rewilded plots. These patterns support previous evidence demonstrating that bacterial communities often reassemble more rapidly than fungi following disturbance (Schmidt et al., 2014; Chen et al., 2021), a possible consequence of shorter generation times and broader metabolic plasticity (Sun et al., 2017). Beta diversity ordinations revealed clear successional shifts in both bacterial and fungal community composition, though their trajectories through ordination space were not tightly aligned. This asynchronous assembly highlights the need, and importance of considering both domains when evaluating microbial responses to restoration.

4.3. Soil chemistry is a key environmental filter for microbial assembly

Generalized dissimilarity modeling showed that soil pH, phosphorus, and carbon were among the strongest predictors of total community turnover, while nitrogen had a strong relationship with only bacterial community structure. Spatial variables explained substantially less variation, underscoring the dominant role of local edaphic conditions tied to rewilding stage in shaping microbial assembly. While chronosequences may be subject to spatially confounding factors, our design minimized such concerns: all plots were in close proximity to each other within a single former monoculture oil palm plantation. Providing further evidence that spatial distance does not confound our results, generalized dissimilarity models showed that geographic distance had little effect on community turnover beyond 100 m, a spatial scale that does not differentiate among our plots. These results strengthen the inference that observed microbial differences primarily reflect rewilding stage rather than spatial heterogeneity.
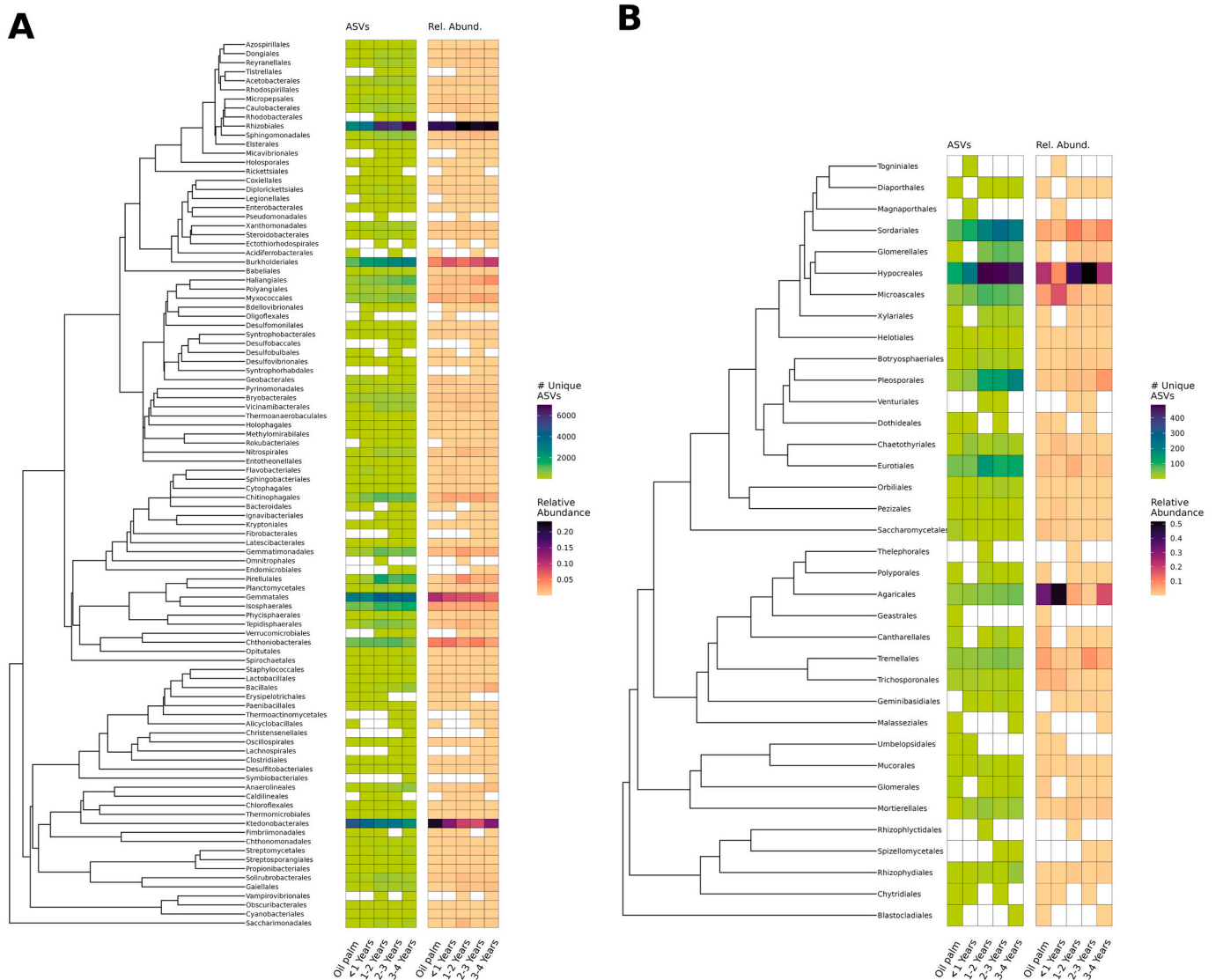
Fig. 8. Bacterial (A) and fungal (B) community across rewilding stages. Left heatmaps (green gradient): Number of unique ASVs within a given order; Right heatmap (red gradient): Mean relative abundance of a given order.

4.4. Network structure reveals divergent temporal dynamics between bacteria and fungi

Ecological network analyses revealed distinct temporal trajectories in microbial community assembly following oil palm rewilding. Bacterial, fungal, and combined networks all show increased complexity and node richness over time, but with differing patterns. Bacterial networks showed progressive increases in clustering coefficient, global efficiency, betweenness, and coreness, indicating a shift toward a highly interconnected and potentially more stable configurations. These patterns are consistent with deterministic assembly processes such as environmental filtering and niche differentiation, which may favor modular structuring and the emergence of central hub taxa.

In contrast, fungal networks displayed an early spike in clustering and betweenness, followed by stabilization, suggesting more rapid initial restructuring. This early restructuring potentially reflects fungal life history traits and their rapid response to new substrates and plant hosts. Many saprotrophic and mycorrhizal (including endophytic) fungi exhibit strong priority effects during early colonization and can rapidly extend mycelial networks, which may lead to a transient increase in connectivity in fungal interaction networks as pioneer lineages establish interactions (Yang et al., 2025). As rewilding progresses, host filtering

may shift the fungal community toward more stable, functionally complementary assemblages, which could underlie the observed stabilization of network topology (Frew et al., 2023). Combined microbial networks expanded in node richness and mean path length but exhibited only modest gains in global efficiency, implying parallel assembly within bacterial and fungal subnetworks rather than strong cross-domain integration.

Together, these results indicate a gradual reassembly of microbial interaction networks over the rewilding chronosequence, marked by increasing connectivity, the reemergence of structural complexity, and domain-specific succession patterns. They provide strong evidence that microbial coalescence during restoration is not a uniform process, but rather reflects the interplay of legacy effects, ecological filters, and domain-specific assembly rules.

While co-occurrence networks remain correlative and cannot confirm specific ecological interactions (Goberna and Verdú, 2022), our use of conservative network inference methods (e.g., SpiecEasi), multiple filters for identifying key taxa, and consistent patterns across rewilding stages support the ecological relevance of the observed shifts. Interpreted alongside soil chemical gradients and compositional turnover, these network changes offer a robust lens into the reorganization of microbial connectivity during rewilding.

Although our study did not directly measure ecosystem processes such as respiration or nutrient fluxes, the observed increase in microbial network connectivity likely reflects enhanced functional integration of the soil community. More connected and modular networks are often associated with greater functional redundancy and stability in microbial systems (Banerjee et al., 2018; Wagg et al., 2019). The rise in bacterial global efficiency and clustering coefficient during rewilding therefore suggests a strengthening of metabolic interdependence and potential resilience to disturbance. Parallel increases in soil carbon, nitrogen, and phosphorus further support the view that rewilding fosters both structural and biogeochemical recovery, linking microbial network reorganization to early improvements in soil function.

4.5. Keystone taxa shift across rewilding stages

Taxa meeting all three criteria for inclusion (identified as hubs, differentially abundant, and strongly predictive of rewilding stage) included members of well-known bacterial and fungal clades. For bacteria, members of Acidobacteria and Verrucomicrobia increased over time and were identified as key predictors of rewilding stage. This is consistent with their roles in nutrient cycling and adaptation to oligotrophic conditions (Kielak et al., 2016; Shen et al., 2017). For fungi, increased representation of ectomycorrhizal and saprotrophic taxa in later-stage rewilded plots supports the idea that plant-microbe associations and decomposition dynamics strengthen during rewilding.

4.6. Implications for microbial assembly theory and restoration ecology

Together, these results highlight the importance of tracking both bacterial and fungal communities and their interactions with soil chemistry during restoration. Our findings support theoretical predictions regarding asynchronous community assembly, the dominant role of environmental filters such as soil nutrients, and the non-uniform nature of community coalescence. The increase in microbial diversity, turnover, and network complexity over the first three years of rewilding suggests that microbial systems can undergo rapid, structured reassembly even in landscapes heavily shaped by industrial agriculture.

The global expansion of oil palm agriculture, particularly in Southeast Asia, has driven extensive tropical deforestation, biodiversity loss, and soil degradation. Malaysia, now the world's second-largest palm oil producer (Ghulam Kadir, 2024), exemplifies the trade-off between commodity-driven land use and ecological resilience. As demand for palm oil continues to grow (Murphy et al., 2021), sustainable strategies that restore soil function and biodiversity while maintaining economic productivity are urgently needed. Rewilding initiatives like the one studied here offer a promising model, demonstrating that even within heavily altered landscapes, microbial communities can begin to recover structure and function within a few years. By identifying key indicators of microbial reassembly, our results contribute to a growing body of work aimed at guiding restoration efforts in tropical agricultural systems toward more biodiverse, resilient, and ecologically integrated outcomes.

Our results align with assembly frameworks that predict a progression from stochastic to deterministic processes during succession (Stegen et al., 2012). Early rewilding stages appear dominated by stochastic dispersal and priority effects, particularly among fungi, leading to transiently complex but unstable networks. As environmental conditions stabilize, deterministic filtering by soil chemistry and host associations promotes more structured, functionally complementary assemblages. These dynamics illustrate how microbial coalescence integrates both stochastic and deterministic forces across time.

4.7. Future work

While the work performed here is valuable and shows how microbial community structure and assembly changes over a 5-year chronosequence, future work should examine multiple rewilding projects to determine whether similar drivers influence rewilding success, soil chemistry changes and microbial community assembly across broad geographic scales. Additionally, the inclusion of plant community data would allow for a more intricate and nuanced examination of microbial community change and assembly dynamics as rewilding advances.

5. Conclusions

We show that microbial communities in tropical agricultural soils underwent structured and domain-specific reassembly within just a few years of rewilding. Bacterial and fungal communities followed distinct successional trajectories, shaped by early shifts in key soil nutrients, with increasing microbial diversity, compositional turnover, and network complexity over time. The emergence of domain-specific network structures and keystone taxa underscores the non-uniform nature of microbial coalescence and highlights the central role of soil chemistry in shaping post-agriculture assembly. These findings reinforce core predictions from community assembly theory, including the dominant role of environmental filtering, asynchronous domain-level succession, and increasing biotic interactions, while offering applied insight into microbial responses to ecological restoration. By leveraging a real rewilding chronosequence in a heavily modified tropical oil palm system, this work fills a critical gap between theoretical models and real-world land-use recovery.

These results offer practical insight into how microbiomes respond to ecological restoration and highlight key microbial indicators that may guide rewilding efforts in degraded tropical landscapes. Future work should examine how these early shifts scale to longer-term trajectories and broader ecosystem recovery, including interactions with plant and faunal communities. As global demand for sustainable land management grows, our results highlight the potential value of microbiome-informed restoration strategies that support biodiversity, resilience, and soil ecosystem function.

CRediT authorship contribution statement

Geoffrey Zahn: Writing – review & editing, Writing – original draft, Visualization, Validation, Software, Methodology, Investigation, Formal analysis, Data curation. **Carl E. Hjelmen:** Writing – review & editing, Visualization, Validation, Formal analysis. **Benjamin J. Wainwright:** Writing – review & editing, Writing – original draft, Visualization, Validation, Supervision, Resources, Project administration, Methodology, Investigation, Funding acquisition, Formal analysis, Data curation, Conceptualization.

Consent for publication

Not applicable.

Ethics approval and consent to participate

Not applicable.

Funding

Declaration of competing interest

The authors declare that they have no competing interests.

Acknowledgements

contributed to the results reported within this paper. We are grateful for the logistical support and assistance with sample collection provided by the staff of A Little Wild Farms (https://alittlewild.com/). We thank Real Impact Advisors (RIA) (https://www.realimpactadvisors.com/) for advice and guidance.

Appendix A. Supplementary data

Supplementary data to this article can be found online at https://doi.org/10.1016/j.scitotenv.2025.180999.

Data availability

The datasets supporting the conclusions of this article are available in the Sequence Read Archive repository, Accession PRJNA1117193 (https://www.ncbi.nlm.nih.gov/bioproject/PRJNA1117193), and the Zenodo repositories (https://zenodo.org/records/14708616) and (https://zenodo.org/doi/10.5281/zenodo.15677641).

References

Ahmad Ali, S.R., Ahmad Tajuddin, N.S., Bakeri, S.A., 2012. Underground microbial biodiversity during conversion of secondary logged over forest for oil palm plantation in Belaga, Sarawak. In: Presented at the UMT 11th International Annual Symposium on Sustainability Science and Management. Terengganu, Malaysia.

Banerjee, S., Schlaeppi, K., van der Heijden, M.G.A., 2018. Keystone taxa as drivers of microbiome structure and functioning. Nat. Rev. Microbiol. 16, 567–576. https://doi.org/10.1038/s41579-018-0024-1.

Callahan, B.J., McMurdie, P.J., Rosen, M.J., Han, A.W., Johnson, A.J.A., Holmes, S.P., 2016. DADA2: High-resolution sample inference from Illumina amplicon data. Nat. Methods 13, 581–583. https://doi.org/10.1038/nmeth.3869.

Chen, J., Zhou, Y., Zhang, Y., 2022. New Insights into Microbial Degradation of Cyanobacterial Organic Matter Using a Fractionation Procedure. Int. J. Environ. Res. Public Health 19, 6981. https://doi.org/10.3390/ijerph19126981.

Chen, M., Zhu, X., Zhao, C., Yu, P., Abulaizi, M., Jia, H., 2021. Rapid microbial community evolution in initial Carex litter decomposition stages in Bayinbuluk alpine wetland during the freeze–thaw period. Ecol. Indic. 121, 107180. https://doi.org/10.1016/j.ecolind.2020.107180.

Csárdi, G., Nepusz, T., Müller, K., Horvát, S., Traag, V., Zanini, F., Noom, D., 2023. Igraph for R: R Interface of the Igraph Library for Graph Theory and Network Analysis. https://doi.org/10.5281/ZENODO.7682609.

Dang, K., Ma, Y., Liang, H., Fan, Z., Guo, S., Li, Z., Li, H., Zhang, S., 2024. Distinct planting patterns exert legacy effects on the networks and assembly of root-associated microbiomes in subsequent crops. Sci. Total Environ. 946, 174276. https://doi.org/10.1016/j.scitotenv.2024.174276.

Davis, N.M., Proctor, D.M., Holmes, S.P., Relman, D.A., Callahan, B.J., 2018. Simple statistical identification and removal of contaminant sequences in marker-gene and metagenomics data. Microbiome 6, 226. https://doi.org/10.1186/s40168-018-0605-2.

De Vries, F.T., Griffiths, R.I., Bailey, M., Craig, H., Girlanda, M., Gweon, H.S., Hallin, S., Kaisermann, A., Keith, A.M., Kretzschmar, M., Lemanceau, P., Lumini, E., Mason, K. E., Oliver, A., Ostle, N., Prosser, J.I., Thion, C., Thomson, B., Bardgett, R.D., 2018. Soil bacterial networks are less stable under drought than fungal networks. Nat. Commun. 9, 3033. https://doi.org/10.1038/s41467-018-05516-7.

Dong, M., Kowalchuk, G.A., Liu, H., Xiong, W., Deng, X., Zhang, N., Li, R., Shen, Q., Dini-Andreote, F., 2021. Microbial community assembly in soil aggregates: A dynamic interplay of stochastic and deterministic processes. Appl. Soil Ecol. 163, 103911. https://doi.org/10.1016/j.apsoil.2021.103911.

Du, Y., Yang, Y., Wu, S., Gao, X., He, X., Dong, S., 2025. Core microbes regulate plant-soil resilience by maintaining network resilience during long-term restoration of alpine grasslands. Nat. Commun. 16, 3116. https://doi.org/10.1038/s41467-025-58080-2.

Fitzpatrick, M., Mokany, K., Manion, G., Nieto-Lugilde, D., Ferrier, S., 2022. gdm: Generalized Dissimilarity Modeling.

Frank, J.A., Reich, C.I., Sharma, S., Weisbaum, J.S., Wilson, B.A., Olsen, G.J., 2008. Critical Evaluation of Two Primers Commonly Used for Amplification of Bacterial 16S rRNA Genes. Appl. Environ. Microbiol. 74, 2461–2470. https://doi.org/10.1128/AEM.02272-07.

Frew, A., Heuck, M.K., Aguilar-Trigueros, C.A., 2023. Host filtering, not competitive exclusion, may be the main driver of arbuscular mycorrhizal fungal community assembly under high phosphorus. Funct. Ecol. 37, 1856–1869. https://doi.org/10.1111/1365-2435.14349.

Fukami, T., 2015. Historical Contingency in Community Assembly: Integrating Niches, Species Pools, and Priority Effects. Annu. Rev. Ecol. Evol. Syst. 46, 1–23. https://doi.org/10.1146/annurev-ecolsys-110411-160340.

Ghulam Kadir, A.P., 2024. Oil palm economic performance in malaysia and R&D progress in 2023. Journal of Oil Palm Research. https://doi.org/10.21894/jopr.2024.0037.

Goberna, M., Verdú, M., 2022. Cautionary notes on the use of co-occurrence networks in soil ecology. Soil Biol. Biochem. 166, 108534. https://doi.org/10.1016/j.soilbio.2021.108534.

Goeker, M., 2022. BacDive: API Client for BacDive.

Greenwell .M., B., Boehmke .C., B., 2020. Variable importance plots—an introduction to the vip package. R J. 12, 343. https://doi.org/10.32614/RJ-2020-013.

Guillaume, T., Holtkamp, A.M., Damris, M., Brümmer, B., Kuzyakov, Y., 2016. Soil degradation in oil palm and rubber plantations under land resource scarcity. Agric. Ecosyst. Environ. 232, 110–118. https://doi.org/10.1016/j.agee.2016.07.002.

Hernández, D.L., Esch, E.H., Alster, C.J., McKone, M.J., Camill, P., 2013. Rapid Accumulation of Soil Carbon and Nitrogen in a Prairie Restoration Chronosequence. Soil Sci. Soc. Am. J. 77, 2029–2038. https://doi.org/10.2136/sssaj2012.0403.

Huang, J., Gao, K., Yang, L., Lu, Y., 2023. Successional action of Bacteroidota and Firmicutes in decomposing straw polymers in a paddy soil. Environmental Microbiome 18, 76. https://doi.org/10.1186/s40793-023-00533-6.

Jiang, S., Xing, Y., Liu, G., Hu, C., Wang, X., Yan, G., Wang, Q., 2021. Changes in soil bacterial and fungal community composition and functional groups during the succession of boreal forests. Soil Biol. Biochem. 161, 108393. https://doi.org/10.1016/j.soilbio.2021.108393.

Jiao, S., Chu, H., Zhang, B., Wei, X., Chen, W., Wei, G., 2022. Linking soil fungi to bacterial community assembly in arid ecosystems. iMeta 1, e2. https://doi.org/10.1002/imt2.2.

Kielak, A.M., Barreto, C.C., Kowalchuk, G.A., Van Veen, J.A., Kuramae, E.E., 2016. The Ecology of Acidobacteria: Moving beyond Genes and Genomes. Front. Microbiol. 7. https://doi.org/10.3389/fmicb.2016.00744.

Kleinberg, J.M., 1999. Authoritative sources in a hyperlinked environment. J. ACM 46, 604–632. https://doi.org/10.1145/324133.324140.

Kurtz, Z., Mueller, C., Miraldi, E., Bonneau, R., 2024. SpiecEasi: Sparse Inverse Covariance for Ecological Statistical Inference.

Kuznetsova, A., Brockhoff, P.B., Christensen, R.H., 2017. LmerTest package: tests in linear mixed effects models. J. Stat. Softw. 82, 1–26.

Li, Y., Steenwyk, J.L., Chang, Y., Wang, Y., James, T.Y., Stajich, J.E., Spatafora, J.W., Groenewald, M., Dunn, C.W., Hittinger, C.T., Shen, X.-X., Rokas, A., 2021. A genome-scale phylogeny of the kingdom Fungi. Curr. Biol. 31, 1653–1665.e5. https://doi.org/10.1016/j.cub.2021.01.074.

Lim, F.K.S., Carrasco, L.R., Edwards, D.P., McHardy, J., 2024. Land-use change from market responses to oil palm intensification in Indonesia. Conserv. Biol. 38, e14149. https://doi.org/10.1111/cobi.14149.

Liu, N., Hu, H., Ma, W., Deng, Y., Wang, Q., Luo, A., Meng, J., Feng, X., Wang, Z., 2021. Relative importance of deterministic and stochastic processes on soil microbial community assembly in temperate grasslands. Microorganisms 9, 1929. https://doi.org/10.3390/microorganisms9091929.

Liu, S., Wang, H., Tian, P., Yao, X., Sun, H., Wang, Q., Delgado-Baquerizo, M., 2020. Decoupled diversity patterns in bacteria and fungi across continental forest ecosystems. Soil Biol. Biochem. 144, 107763. https://doi.org/10.1016/j.soilbio.2020.107763.

Lozupone, C., Lladser, M.E., Knights, D., Stombaugh, J., Knight, R., 2011. UniFrac: an effective distance metric for microbial community comparison. ISME J. 5, 169–172. https://doi.org/10.1038/ismej.2010.133.

Martin, B., Witten, D., Willis, A., 2022. corncob: Count regression for Correlated Observations with the Beta-Binomial.

Martin, M., 2011. Cutadapt removes adapter sequences from high-throughput sequencing reads. EMBnet.Journal 17, 10–12. https://doi.org/10.14806/ej.17.1.200.

Mazzella, V., Zahn, G., Dell'Anno, A., Pons, L.N., 2025. Marine Mycobiomes Colonize Mediterranean Sponge Hosts in a Random Fashion. Microb. Ecol. 88, 25. https://doi.org/10.1007/s00248-025-02523-2.

McDonald, D., Jiang, Y., Balaban, M., Cantrell, K., Zhu, Q., Gonzalez, A., Morton, J.T., Nicolaou, G., Parks, D.H., Karst, S.M., Albertsen, M., Hugenholtz, P., DeSantis, T., Song, S.J., Bartko, A., Havulinna, A.S., Jousilahti, P., Cheng, S., Inouye, M., Niiranen, T., Jain, M., Salomaa, V., Lahti, L., Mirarab, S., Knight, R., 2024. Greengenes2 unifies microbial data in a single reference tree. Nat. Biotechnol. 42, 715–718. https://doi.org/10.1038/s41587-023-01845-1.

McMurdie, P.J., Holmes, S., 2013. phyloseq: An R Package for Reproducible Interactive Analysis and Graphics of Microbiome Census Data. PLoS One 8, e61217. https://doi.org/10.1371/journal.pone.0061217.

Mittelman, P., Landim, A.R., Genes, L., Assis, A.P.A., Starling-Manne, C., Leonardo, P.V., Fernandez, F.A.S., Guimarães Jr., P.R., Pires, A.S., 2022. Trophic rewilding benefits a tropical community through direct and indirect network effects. Ecography 2022. https://doi.org/10.1111/ecog.05838 ecog.05838.

Morrison, M.L., Xue, K.S., Rosenberg, N.A., 2025. Quantifying compositional variability in microbial communities with FAVA. Proc. Natl. Acad. Sci. 122, e2413211122. https://doi.org/10.1073/pnas.2413211122.

Murphy, D.J., Goggin, K., Paterson, R.R.M., 2021. Oil palm in the 2020s and beyond: challenges and solutions. CABI Agric. Biosci. 2, 39. https://doi.org/10.1186/s43170-021-00058-3.

Oksanen, J., Simpson, G.L., Blanchet, F.G., Kindt, R., Legendre, P., Minchin, P.R., O'Hara, R.B., Solymos, P., Stevens, M.H.H., Szoecs, E., Wagner, H., Barbour, M., Bedward, M., Bolker, B., Borcard, D., Carvalho, G., Chirico, M., Caceres, M.D., Durand, S., Evangelista, H.B.A., FitzJohn, R., Friendly, M., Furneaux, B., Hannigan, G., Hill, M.O., Lahti, L., McGlinn, D., Ouellette, M.-H., Cunha, E.R., Smith, T., Stier, A., Braak, C.J.F.T., Weedon, J., Borman, T., 2025. vegan: Community Ecology Package.

Paulitz, T.C., Menge, J.A., 1984. Is Spizellomyces Punctatum a Parasite or Saprophyte of Vesicular-Arbuscular Mycorrhizal Fungi? Mycologia 76, 99–107. https://doi.org/10.1080/00275514.1984.12023813.

Peng, Z., Qian, X., Liu, Y., Li, X., Gao, H., An, Y., Qi, J., Jiang, L., Zhang, Y., Chen, S., Pan, H., Chen, B., Liang, C., Van Der Heijden, M.G.A., Wei, G., Jiao, S., 2024. Land conversion to agriculture induces taxonomic homogenization of soil microbial

communities globally. Nat. Commun. 15, 3624. https://doi.org/10.1038/s41467-024-47348-8.

Quast, C., Pruesse, E., Yilmaz, P., Gerken, J., Schweer, T., Yarza, P., Peplies, J., Glöckner, F.O., 2013. The SILVA ribosomal RNA gene database project: improved data processing and web-based tools. Nucleic Acids Res. 41, D590–D596. https://doi.org/10.1093/nar/gks1219.

R Core Team, 2024. R: A Language and Environment for Statistical Computing. R Foundation for Statistical Computing, Vienna, Austria.

Rillig, M.C., Antonovics, J., Caruso, T., Lehmann, A., Powell, J.R., Veresoglou, S.D., Verbruggen, E., 2015. Interchange of entire communities: microbial community coalescence. Trends Ecol. Evol. 30, 470–476. https://doi.org/10.1016/j.tree.2015.06.004.

Saltonstall, K., van Breugel, M., Navia, W., Castillo, H., Hall, J.S., 2025. Soil microbial communities in dry and moist tropical forests exhibit distinct shifts in community composition but not diversity with succession. Microbiol. Spectr. 13, e0193124. https://doi.org/10.1128/spectrum.01931-24.

Schliep, K.P., 2011. phangorn: phylogenetic analysis in R. Bioinformatics 27, 592–593. https://doi.org/10.1093/bioinformatics/btq706.

Schmidt, S.K., Nemergut, D.R., Darcy, J.L., Lynch, R., 2014. Do bacterial and fungal communities assemble differently during primary succession? Mol. Ecol. 23, 254–258. https://doi.org/10.1111/mec.12589.

Shen, C., Ge, Y., Yang, T., Chu, H., 2017. Verrucomicrobial elevational distribution was strongly influenced by soil pH and carbon/nitrogen ratio. J. Soils Sediments 17, 2449–2456. https://doi.org/10.1007/s11368-017-1680-x.

Shen, C., Gunina, A., Luo, Y., Wang, J., He, J., Kuzyakov, Y., Hemp, A., Classen, A.T., Ge, Y., 2020a. Contrasting patterns and drivers of soil bacterial and fungal diversity across a mountain gradient. Environ. Microbiol. 22, 3287–3301. https://doi.org/10.1111/1462-2920.15090.

Shen, M., Zhang, J.Q., Zhao, L.L., Groenewald, J.Z., Crous, P.W., Zhang, Y., 2020b. Venturiales. Stud. Mycol. 96, 185–308. https://doi.org/10.1016/j.simyco.2020.03.001.

Silverstein, M.R., Segrè, D., Bhatnagar, J.M., 2023. Environmental microbiome engineering for the mitigation of climate change. Glob. Chang. Biol. 29, 2050–2066. https://doi.org/10.1111/gcb.16609.

Stegen, J.C., Lin, X., Konopka, A.E., Fredrickson, J.K., 2012. Stochastic and deterministic assembly processes in subsurface microbial communities. ISME J. 6, 1653–1664. https://doi.org/10.1038/ismej.2012.22.

Sun, S., Li, S., Avera, B.N., Strahm, B.D., Badgley, B.D., 2017. Soil Bacterial and Fungal Communities Show Distinct Recovery Patterns during Forest Ecosystem Restoration. Appl. Environ. Microbiol. 83. https://doi.org/10.1128/AEM.00966-17 e00966–17.

Tedersoo, L., Anslan, S., 2019. Towards PacBio-based pan-eukaryote metabarcoding using full-length ITS sequences. Environ. Microbiol. Rep. 11, 659–668. https://doi.org/10.1111/1758-2229.12776.

Tedersoo, L., Hosseyni Moghaddam, M.S., Mikryukov, V., Hakimzadeh, A., Bahram, M., Nilsson, R.H., Yatsiuk, I., Geisen, S., Schwelm, A., Piwosz, K., Prous, M., Sildever, S., Chmolowska, D., Rueckert, S., Skaloud, P., Laas, P., Tines, M., Jung, J.-H., Choi, J.H., Alkahtani, S., Anslan, S., 2024. EUKARYOME: the rRNA gene reference database for identification of all eukaryotes. Database 2024, baae043. https://doi.org/10.1093/database/baae043.

Tsiafouli, M.A., Thébault, E., Sgardelis, S.P., De Ruiter, P.C., Van Der Putten, W.H., Birkhofer, K., Hemerik, L., De Vries, F.T., Bardgett, R.D., Brady, M.V., Bjornlund, L., Jørgensen, H.B., Christensen, S., Hertefeldt, T.D., Hotes, S., Gera Hol, W.H., Frouz, J., Liiri, M., Mortimer, S.R., Setälä, H., Tzanopoulos, J., Uteseny, K., Pižl, V., Stary, J., Wolters, V., Hedlund, K., 2015. Intensive agriculture reduces soil biodiversity across Europe. Glob. Chang. Biol. 21, 973–985. https://doi.org/10.1111/gcb.12752.

Turner, E.C., Snaddon, J.L., Fayle, T.M., Foster, W.A., 2008. Oil Palm Research in Context: Identifying the Need for Biodiversity Assessment. PLoS One 3, e1572. https://doi.org/10.1371/journal.pone.0001572.

Van Der Heijden, M.G.A., Bardgett, R.D., Van Straalen, N.M., 2008. The unseen majority: soil microbes as drivers of plant diversity and productivity in terrestrial ecosystems. Ecol. Lett. 11, 296–310. https://doi.org/10.1111/j.1461-0248.2007.01139.x.

Van Der Putten, W.H., Bardgett, R.D., Bever, J.D., Bezemer, T.M., Casper, B.B., Fukami, T., Kardol, P., Klironomos, J.N., Kulmatiski, A., Schweitzer, J.A., Suding, K. N., Van De Voorde, T.F.J., Wardle, D.A., 2013. Plant–soil feedbacks: the past, the present and future challenges. J. Ecol. 101, 265–276. https://doi.org/10.1111/1365-2745.12054.

Wagg, C., Schlaeppi, K., Banerjee, S., Kuramae, E.E., van der Heijden, M.G.A., 2019. Fungal-bacterial diversity and microbiome complexity predict ecosystem functioning. Nat. Commun. 10, 4841. https://doi.org/10.1038/s41467-019-12798-y.

Wainwright, B.J., Zahn, G.L., Afiq-Rosli, L., Tanzil, J.T.I., Huang, D., 2020. Host age is not a consistent predictor of microbial diversity in the coral Porites lutea. Sci. Rep. 10, 14376. https://doi.org/10.1038/s41598-020-71117-4.

Wei, H., Deng, Y., Lin, L., Wang, J., Huang, J., 2023. Improved soil composition promotes nutrient recovery during vegetation restoration in karst peak-cluster depressions. CATENA 222, 106769. https://doi.org/10.1016/j.catena.2022.106769.

Wright, E.S., 2016. Using DECIPHER v2.0 to Analyze Big Biological Sequence Data in R. R Journal 8, 352–359.

Wright, M.N., Ziegler, A., 2017. ranger : A Fast Implementation of Random Forests for High Dimensional Data in C++ and R. J. Stat. Softw. 77. https://doi.org/10.18637/jss.v077.i01.

Yang, D., He, Z., Lin, Y., He, X., Kong, X., 2025. Priority colonization of endophytic fungal strains drives litter decomposition and saprotroph assembly via functional trait selection in karst oak forests. Microorganisms 13, 1066. https://doi.org/10.3390/microorganisms13051066.

Zahn, G., 2024a. gzahn/mycobank: alpha_version. https://doi.org/10.5281/ZENODO.10439638.

Zahn, G., 2024b. Hubfindr R Package: Identifying Keystone Taxa in Co-Occurrence Networks. https://doi.org/10.5281/ZENODO.12741089.

Zahn, G., Amend, A.S., 2019. Foliar fungi alter reproductive timing and allocation in Arabidopsis under normal and water-stressed conditions. Fungal Ecol. 41, 101–106. https://doi.org/10.1016/j.funeco.2019.04.002.

Zahn, Geoffrey, Hjelmen, Carl, 2025. gzahn/Palm_Oil_Recovery: 1.0. https://doi.org/10.5281/ZENODO.15677641.